Stability analysis of amplitude death in delay-coupled high-dimensional map networks and their design procedure

著者	Watanabe Tomohiko, Sugitani Yoshiki, Konishi Keiji, Hara Naoyuki
journal or publication title	Physica D: Nonlinear Phenomena
volume	338
page range	26-33
year	2017-01-01
権利	(C) 2017. This manuscript version is made available under the CC-BY-NC-ND 4.0 license http://creativecommons.org/licenses/by-nc-nd/4.0/
URL	http://hdl.handle.net/10466/00017040

doi: https://doi.org/10.1016/j.physd.2016.07.011

Stability analysis of amplitude death in delay-coupled high-dimensional map networks and their design procedure

Tomohiko Watanabe[a], Yoshiki Sugitani[b], Keiji Konishi[a,*], Naoyuki Hara[a]

[a] *Department of Electrical and Information Systems, Osaka Prefecture University*
1–1 Gakuen-cho, Naka-ku, Sakai, Osaka 599-8531 Japan
[b] *Department of Electrical and Electronic Engineering, Ibaraki University*
4–12–1 Nakanarusawa, Hitachi, Ibaraki 316-8511 Japan

Abstract

The present paper studies amplitude death in high-dimensional maps coupled by time-delay connections. A linear stability analysis provides several sufficient conditions for an amplitude death state to be unstable, i.e., an odd number property and its extended properties. Furthermore, necessary conditions for stability are provided. These conditions, which reduce trial-and-error tasks for design, and the convex direction, which is a popular concept in the field of robust control, allow us to propose a design procedure for system parameters, such as coupling strength, connection delay, and input-output matrices, for a given network topology. These analytical results are confirmed numerically using delayed logistic maps, generalized Henon maps, and piecewise linear maps.

Keywords: Time delay, Amplitude death, Map networks, Delay connections, Design procedure, Convex direction

1. Introduction

A considerable number of studies have examined various phenomena in coupled continuous-time nonlinear oscillators [1–4] and coupled discrete-time nonlinear maps [5, 6]. These phenomena are roughly classified into two types: weak- and strong-coupling induced phenomena. For weak coupling, the phases of coupled oscillators are governed by simple phase dynamics [7, 8], and for strong coupling, their amplitudes are influenced by connections. Amplitude death, a phenomenon that occurs with strong coupling, has been widely investigated both analytically and experimentally [9, 10]. This phenomenon is defined as a stabilization of unstable fixed points embedded within continuous-time nonlinear oscillators with diffusive connections. As this phenomenon can suppress oscillations, it has potential use in the avoidance of undesired oscillations for practical coupled systems [11–13]. However, diffusive connections, the most popular connections, never induce amplitude death in *identical* oscillators [14, 15]. This fact is considered a drawback in terms of utilization of amplitude death.

It is well known that at least three types of connections can overcome this drawback: time-delay [16, 17], dynamics [18–20], and conjugate connections [21]. Among these connections, there has been a gradual accumulation of analytical and experimental knowledge on *time-delay* induced amplitude death [16, 17, 22–25] because the transmission delays of information signals passing through connections [26, 27] are ubiquitous in real situations. Many studies have examined time-delay induced death of coupled *continuous-time* oscillators [9, 10]. Conversely, there have been several efforts to deal with amplitude death in coupled *discrete-time* maps.

Time-delay-induced amplitude death of coupled *discrete-time* maps was reported in 2003 [28]. That study provided analytical results on death in *a pair of high-dimensional* maps with a delayed connection. The results are summarized as follows: (a) death cannot occur with no-delay connections; (b) the odd number property [15] exists even in a pair of high-dimensional maps; and (c) death cannot occur even with delay connections in a pair of *one*-dimensional maps. Result (b) was extended to *a simple ring lattice* [29]. Atay and Karabacak analytically investigated amplitude death in *one*-dimensional map *networks* with *uniform* delay time [30]. Masoller and Martí found amplitude death in one-dimensional map networks with *non-uniform* delay time [31], and the results were investigated analytically and numerically in detail [32–35]. However, few studies have attempted to deal with *high*-dimensional map *networks* [36] because it is not easy to analytically investigate their stability.

This study considers amplitude death in *high*-dimensional map *networks* with *uniform* delay time. We can deal with complex network topologies in the same manner as a simple topology. It is shown that the linear stability of amplitude death is governed by a characteristic equation with topology parameters. The characteristic equation reveals that results (a) and (b) in the previous study [28] for a pair of maps remain even for map networks. As the number of topology parameters is equivalent to that of maps in a network, one may think that a design of connection parameters in networks with a large number of maps is a complicated problem. However, we demonstrate that the convex direction [37], a strong mathematical concept for robust control theory, simplifies the design of connection param-

*Corresponding author
Email address: konishi@eis.osakafu-u.ac.jp (Keiji Konishi)
URL: http://www.eis.osakafu-u.ac.jp/~ecs/index-e.html (Keiji Konishi)

eters. We provide a systematic procedure that designs connection parameters (i.e., coupling strength and connection delay) and the input-output matrices of maps. Furthermore, result (b) is extended to reduce the number of trial-and-error tasks in the design procedure. The analytical results are confirmed numerically using three types of map networks, i.e., delayed logistic [38, 39], generalized Henon [40], and piecewise linear [41, 42] map networks. This paper is a substantially extended version of our previous conference paper [36].

2. Map networks

Consider the following high-dimensional maps,

$$\begin{cases} \boldsymbol{x}_i(n+1) &= \boldsymbol{F}\left[\boldsymbol{x}_i(n)\right] + \boldsymbol{b}u_i(n), \\ y_i(n) &= \boldsymbol{c}\boldsymbol{x}_i(n), \end{cases} \quad (i = 1, \ldots, N), \quad (1)$$

where $\boldsymbol{x}_i(n) \in \mathbb{R}^m$ is the system state of the i-th m-dimensional map at time $n \in \mathbb{Z}$. The input and output signals are $u_i(n) \in \mathbb{R}$ and $y_i(n) \in \mathbb{R}$, respectively. $N \in \mathbb{Z}^+$ represents the number of maps. $\boldsymbol{F} : \mathbb{R}^m \to \mathbb{R}^m$ denotes the nonlinear map, which has at least one fixed point $\boldsymbol{x}^* : \boldsymbol{x}^* = \boldsymbol{F}\left[\boldsymbol{x}^*\right]$. The input and output matrices are $\boldsymbol{b} \in \mathbb{R}^m$ and $\boldsymbol{c} \in \mathbb{R}^{1\times m}$, respectively. Here, the input signal $u_i(n)$ with connection delay $\tau \in \mathbb{Z}^+$and coupling strength $k \in \mathbb{R}$ is expressed as follows:

$$u_i(n) = k\left[\left\{\sum_{l=1}^{N} \frac{\varepsilon_{il}}{d_i} y_l(n-\tau)\right\} - y_i(n)\right], \quad (2)$$

$$d_i := \sum_{l=1}^{N} \varepsilon_{il},$$

where ε_{il} governs the network topology. Here, $\varepsilon_{il} = \varepsilon_{li} = 1$ $(= 0)$ indicates that maps i and l are (are not) connected. In addition, self-feedback is not allowed (i.e., $\varepsilon_{ii} = 0$). The number of maps connected to map i is expressed by d_i.

Here we focus on the following spatial uniform equilibrium state of map network (1) with connection delay (2):

$$\left[\boldsymbol{x}_1(n)^T \quad \cdots \quad \boldsymbol{x}_N(n)^T\right]^T = \left[\boldsymbol{x}^{*T} \quad \cdots \quad \boldsymbol{x}^{*T}\right]^T. \quad (3)$$

The linearized dynamics of a coupled map network (1) (2) at equilibrium state (3) is described as follows:

$$\boldsymbol{v}_i(n+1) = (\boldsymbol{A} - k\boldsymbol{b}\boldsymbol{c})\,\boldsymbol{v}_i(n) + k\boldsymbol{b}\boldsymbol{c}\sum_{l=1}^{N} \frac{\varepsilon_{il}}{d_i}\boldsymbol{v}_l(n-\tau), \quad (4)$$

$$\boldsymbol{A} := \left.\frac{\partial \boldsymbol{F}(\boldsymbol{x})}{\partial \boldsymbol{x}}\right|_{\boldsymbol{x}=\boldsymbol{x}^*}, \quad (5)$$

where $\boldsymbol{v}_i(n) := \boldsymbol{x}_i(n) - \boldsymbol{x}^*$. Here we employ the following assumption.

Assumption 1. *The fixed point $\boldsymbol{x}^*$ of each isolated map is unstable, i.e., the Jacobi matrix $\boldsymbol{A}$ is unstable. Furthermore, $(\boldsymbol{A}, \boldsymbol{b}, \boldsymbol{c})$ is assumed to be minimal*[1].

Linearized system (4) can be rewritten as follows:

$$\boldsymbol{V}(n+1) = \left[\boldsymbol{I}_N \otimes (\boldsymbol{A} - k\boldsymbol{b}\boldsymbol{c})\right]\boldsymbol{V}(n) + (\boldsymbol{E} \otimes k\boldsymbol{b}\boldsymbol{c})\boldsymbol{V}(n-\tau), \quad (6)$$

where $\boldsymbol{V}(n)$ and $\boldsymbol{E}$ are defined as

$$\boldsymbol{V}(n) := \begin{bmatrix} \boldsymbol{v}_1(n) \\ \vdots \\ \boldsymbol{v}_N(n) \end{bmatrix}, \; \boldsymbol{E} := \begin{bmatrix} \varepsilon_{11}/d_1 & \cdots & \varepsilon_{1N}/d_1 \\ \vdots & \ddots & \vdots \\ \varepsilon_{N1}/d_N & \cdots & \varepsilon_{NN}/d_N \end{bmatrix}.$$

Here the matrix $\boldsymbol{I}_N$ and the symbol $\otimes$ denote an N-dimensional identity matrix and the Kronecker product, respectively. Note that the stability of spatial uniform equilibrium state (3) is equal to that of the mN-dimensional linear system (6) with delay time τ. Substituting a solution $\boldsymbol{V}(n) = z^n\boldsymbol{a}$, with a nonzero vector $\boldsymbol{a} \in \mathbb{R}^{mN}$, into a linearized system (6) allows us to obtain its characteristic polynomial,

$$\bar{G}(z) := \det\left[z\boldsymbol{I}_{mN} - \boldsymbol{I}_N \otimes (\boldsymbol{A} - k\boldsymbol{b}\boldsymbol{c}) - (\boldsymbol{E} \otimes k\boldsymbol{b}\boldsymbol{c})z^{-\tau}\right], \quad (7)$$

which can be used to investigate the stability of equilibrium state (3). We can diagonalize the matrix $\boldsymbol{I}_N - \boldsymbol{E}$ using a matrix $\boldsymbol{T}$ [30, 44] as follows:

$$\boldsymbol{T}^{-1}(\boldsymbol{I}_N - \boldsymbol{E})\boldsymbol{T} = \mathrm{diag}(\rho_1, \ldots, \rho_N). \quad (8)$$

Note that the eigenvalues of $\boldsymbol{I}_N - \boldsymbol{E}$, i.e., ρ_i $(i = 1, \ldots, N)$, satisfy

$$0 = \rho_1 \leq \rho_2 \leq \cdots \leq \rho_N \leq 2, \quad (9)$$

for any number of maps and topology [30]. This diagonalization simplifies characteristic polynomial (7), i.e.,

$$\bar{G}(z) := \prod_{q=1}^{N} \bar{g}(z, \rho_q), \quad (10)$$

$$\bar{g}(z, \rho) := d(z) + kn(z)\left\{1 - (1-\rho)z^{-\tau}\right\}. \quad (11)$$

Here $n(z)$ and $d(z)$ defined as

$$\frac{n(z)}{d(z)} := \boldsymbol{c}(z\boldsymbol{I}_m - \boldsymbol{A})^{-1}\boldsymbol{b} = \frac{\boldsymbol{c}\,\mathrm{adj}(z\boldsymbol{I}_m - \boldsymbol{A})\boldsymbol{b}}{\det\left[z\boldsymbol{I}_m - \boldsymbol{A}\right]}, \quad (12)$$

represent the transfer function of each map (1) from $u_i(n)$ to $y_i(n)$ around the fixed point $\boldsymbol{x}^*$. Note that $n(z)$ and $d(z)$ depend only on each isolated map (i.e., $\boldsymbol{A}, \boldsymbol{b}, \boldsymbol{c}$) but not on connection (2), i.e., k, ε_{il}, and τ. We summarize the above analytical argument as follows.

Lemma 1. *The local stability of spatial uniform equilibrium state (3) of map network (1) (2) is equivalent to the stability of*

[1] $(\boldsymbol{A}, \boldsymbol{b}, \boldsymbol{c})$ is minimal if and only if they are controllable and observable [43]; they can be easily checked numerically.

the following polynomial:

$$G(z) := \prod_{q=1}^{N} g(z, \rho_q), \tag{13}$$

$$g(z, \rho) := z^{\tau} d(z) + kn(z)\,(z^{\tau} - 1 + \rho)\,. \tag{14}$$

Proof. The above argument reveals that the local stability of state (3) is governed by polynomial (10). Since the roots z of $\bar{g}(z, \rho) = 0$ are the same as those of $g(z, \rho) = 0$, the stability of $\bar{g}(z, \rho)$ is equivalent to that of $g(z, \rho)$. As a result, the stability of polynomial (10) is equivalent to that of polynomial (13). □

This study investigates the characteristic polynomial $G(z)$ in Lemma 1 to analyze the stability of equilibrium state (3). It must be emphasized that we perform linear stability analysis around equilibrium state (3). Thus, our analytical results are valid for only the local dynamics around it, i.e., we do not deal with global dynamics. This indicates that, even if the characteristic polynomial $G(z)$ is stable, the states $\boldsymbol{x}_i$ $(i = 1, \ldots, N)$ do not always converge to equilibrium state (3).

3. Stability analysis

This section shows several stability conditions for equilibrium state (3) on the basis of the analysis of $N(m + \tau)$-order polynomial $G(z)$ in Eq. (13). Two types of stability conditions are key points in understanding this section. The first is a *sufficient* condition for state (3) to be unstable. This means that if the sufficient condition is satisfied, the state is unstable; however, if the state is unstable, the sufficient condition is not always satisfied. The second is a *necessary* condition for state (3) to be stable. This means that if the state is stable, then the necessary condition is satisfied; however, if the necessary condition is satisfied, the state is not always stable.

3.1. Unstable conditions

We show a sufficient condition when $\tau = 0$.

Lemma 2. *For connection (2) without delay (i.e., $\tau = 0$), equilibrium state (3) is not stabilized for any $\boldsymbol{E}$, k, $\boldsymbol{b}$, and $\boldsymbol{c}$.*

Proof. Polynomial (13) always includes $g(z, 0) = d(z)$ because $\rho_1 = 0$ holds for any topology. From Eq. (12), we see that $d(z)$ is the characteristic polynomial of matrix $\boldsymbol{A}$, which is assumed to be unstable in Assumption 1. Thus, polynomial (13) is unstable and independent of $\boldsymbol{E}$, k, $\boldsymbol{b}$, and $\boldsymbol{c}$. □

Note that the lemma for $N = 2$ was reported in a previous study [28]. Here, to simplify several proofs that will be introduced below, we provide a preliminary fact.

Lemma 3. *Consider a matrix $\boldsymbol{P} \in \mathbb{R}^{m \times m}$ and its characteristic polynomial $p(z) := \det\left[z\boldsymbol{I}_m - \boldsymbol{P}\right]$. For a real number $z_0 \in \mathbb{R}$ that is not an eigenvalue of $\boldsymbol{P}$, inequality $p(z_0) < 0$ ($p(z_0) > 0$) implies that $\boldsymbol{P}$ has an odd (even) number of real eigenvalues[2] greater than z_0.*

[2] Throughout this paper, the term for real eigenvalues greater than z_0 expresses that the real eigenvalues are within the range $(z_0, +\infty)$.

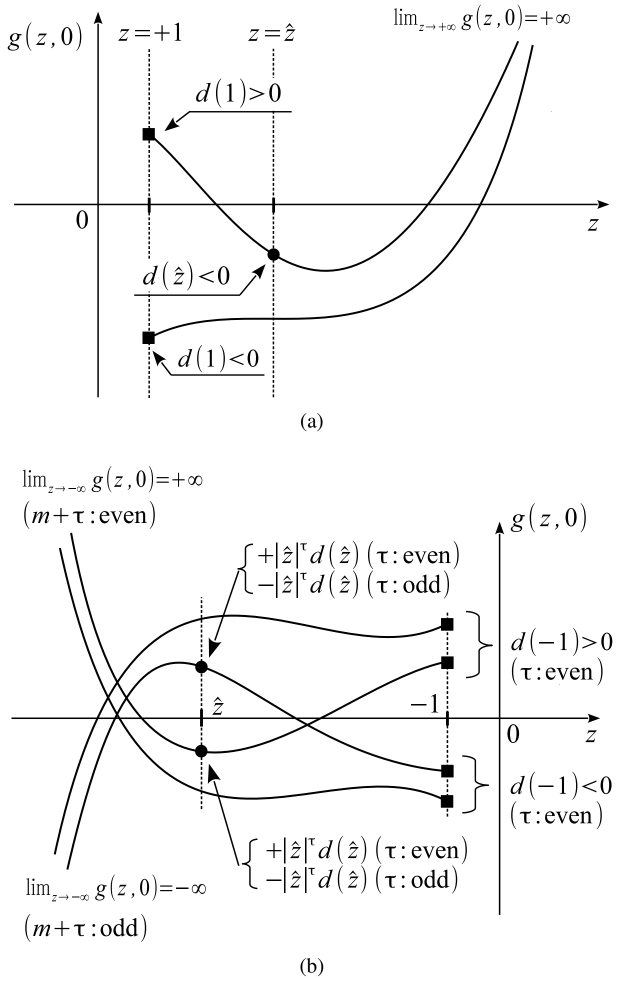

Figure 1: Sketches of characteristic polynomial $g(z, 0)$ for proofs: (a) Theorem 1 and Corollary 1; (b) Theorem 2 and Corollary 2

Proof. $p(z)$ at $z = z_0$ can be rewritten as follows:

$$p(z_0) = \det\left[z_0\boldsymbol{I}_m - \boldsymbol{P}\right] = \prod_{l=1}^{m} \{z_0 - \lambda_l(\boldsymbol{P})\}\,,$$

where $\lambda_l(\boldsymbol{P})$ represents an eigenvalue of $\boldsymbol{P}$. This equation suggests that under the assumption of $z_0 \neq \lambda_l(\boldsymbol{P})$ for any $l \in \{1, \ldots, m\}$, we have $p(z_0) < 0$ ($p(z_0) > 0$) if and only if there exist an odd (even) number of eigenvalues on the real axis greater than z_0. □

Let us consider a sufficient condition under which equilibrium state (3) cannot be stabilized. This is referred to as the odd number property.

Theorem 1. *Equilibrium state (3) is not stabilized for any $\boldsymbol{E}$, k, τ, $\boldsymbol{b}$, and $\boldsymbol{c}$ if an odd number of eigenvalues of the Jacobi matrix $\boldsymbol{A}$ defined by Eq. (5) are on the real axis and are greater than one.*

Proof. $G(z)$ includes $g(z, 0)$ due to $\rho_1 = 0$; thus, this proof focuses only on the stability of $g(z, 0)$. Since $g(z, 0)$ is a $(m + \tau)$-order polynomial of z (see Eq. (14)), then $\lim_{z\to+\infty} g(z, 0) = +\infty$

always holds (Fig. 1(a)). Therefore, if $g(1,0) = d(1) < 0$ holds, we have at least one real root $z > 1$ of $g(z,0) = 0$. From Lemma 3, $d(1) < 0$ suggests that an odd number of eigenvalues of the matrix $\boldsymbol{A}$ are on the real axis and are greater than one. □

Theorem 1 is an extended version of the odd number property of a single map [45, 46], a pair of maps [28], and a simple ring lattice [29] for generalized topologies. Note that Theorem 1 provides no information for which $\boldsymbol{A}$ has an even number of eigenvalues on the real axis that are greater than one. More information is provided in Corollary 1.

Corollary 1. *Let $n(\hat{z}) = 0$ have a solution $\hat{z}$. Equilibrium state (3) is not stabilized for any $\boldsymbol{E}$, k, and τ if there exists at least one $\hat{z} > 1$ such that an odd number of eigenvalues of the matrix $\boldsymbol{A}$ are on the real axis and are greater than $\hat{z}$.*

Proof. In accordance with Theorem 1, we focus on the stability of polynomial $g(z,0)$. This polynomial at $z = \hat{z} > 1$ is reduced to a simple polynomial $g(\hat{z},0) = \hat{z}^{\tau} d(\hat{z})$ due to $n(\hat{z}) = 0$. Here we see that $\lim_{z\to+\infty} g(z,0) = +\infty$ always holds (Fig. 1(a)). Thus, $g(z,0) = 0$ has at least one real root $z > \hat{z} > 1$, if we find at least one $\hat{z} > 1$ such that $g(\hat{z},0) < 0 \Leftrightarrow d(\hat{z}) < 0$ holds. From Lemma 3, the condition $d(\hat{z}) < 0$ implies that an odd number of eigenvalues of the matrix $\boldsymbol{A}$ are on the real axis and are greater than $\hat{z} > 1$. □

Corollary 1 generalizes a previous study [46] that dealt with only a single map.

The above analytical results and the previous related studies focused on only real eigenvalues greater than one. Furthermore, they do not depend on the system dimension m and delay time τ. Here we provide two sufficient unstable conditions based on the real eigenvalues greater than -1 that are dependent on m and τ.

Theorem 2. *Assume that τ is an even number. For an even (odd) m, equilibrium state (3) is not stabilized for any $\boldsymbol{E}$, k, $\boldsymbol{b}$, and $\boldsymbol{c}$ if an odd (even) number of eigenvalues of the matrix $\boldsymbol{A}$ are on the real axis and are greater than -1.*

Proof. Let us analyze the stability of $g(z,0)$ as well as Theorem 1. If $m + \tau$ is an even (odd) number, we have $\lim_{z\to-\infty} g(z,0) = +\infty$ $(= -\infty)$ due to the highest order $m+\tau$ of $g(z,0)$ (Fig. 1(b)). Furthermore, for an even τ, we see that $g(-1,0) = d(-1)$. These facts provide the following results. For an even $m+\tau$ and even τ (i.e., an even m and even τ), $g(z,0) = 0$ has at least one real root $z < -1$ if $g(-1,0) = d(-1) < 0$ holds. The condition $d(-1) < 0$ suggests that an odd number of eigenvalues of the matrix $\boldsymbol{A}$ are on the real axis and are greater than -1. For an odd $m + \tau$ and even τ (i.e., an odd m and even τ), $g(z,0) = 0$ has at least one real root $z < -1$ if $g(-1,0) = d(-1) > 0$ holds. The condition $d(-1) > 0$ suggests that an even number of eigenvalues of the matrix $\boldsymbol{A}$ are on the real axis and are greater than -1. □

Corollary 2. *Let $\hat{z}$ be a solution of $n(\hat{z}) = 0$. For an even (odd) m, equilibrium state (3) is not stabilized for any $\boldsymbol{E}$, k, and τ if there exists at least one $\hat{z} < -1$ such that an odd (even) number of eigenvalues of the matrix $\boldsymbol{A}$ are on the real axis and are greater than $\hat{z}$.*

Proof. Here, the stability of $g(z,0)$ is analyzed as well as Theorem 1. As with Theorem 2, we have $\lim_{z\to-\infty} g(z,0) = +\infty$ $(= -\infty)$ for an even (odd) $m + \tau$ (Fig. 1(b)). Furthermore, for an even (odd) τ, we see that $g(\hat{z},0) = (\hat{z})^{\tau} d(\hat{z}) = +|\hat{z}|^{\tau} d(\hat{z})$ $(= -|\hat{z}|^{\tau} d(\hat{z}))$. Therefore, for an even $m + \tau$, if we find at least one $\hat{z} < -1$ such that $d(\hat{z}) < 0$ with an even τ or $d(\hat{z}) > 0$ with an odd τ hold, then at least one real root $z < \hat{z} < -1$ of $g(z,0) = 0$ exists. In addition, for an odd $m + \tau$, if we find at least one $\hat{z} < -1$ such that $g(\hat{z},0) = +|\hat{z}|^{\tau} d(\hat{z}) > 0$ with an even τ or $g(\hat{z},0) = -|\hat{z}|^{\tau} d(\hat{z}) > 0$ with an odd τ hold, then at least one real root $z < \hat{z} < -1$ of $g(z,0) = 0$ exists. These facts are summarized as follows. At least one real root $z < \hat{z} < -1$ of $g(z,0) = 0$ exists if $d(\hat{z}) < 0$ with an even m holds or $d(\hat{z}) > 0$ with an odd m holds. From Lemma 3, the inequality $d(\hat{z}) < 0$ (> 0) implies that an odd (even) number of eigenvalues of the matrix $\boldsymbol{A}$ are on the real axis and are greater than $\hat{z} < -1$. □

It must be emphasized that Theorem 2 and Corollary 2 have not been introduced in previous studies, even for $N = 1, 2$. These sufficient conditions reduce the number of trial-and-error tasks when designing connections, because we know that if at least one of these conditions holds, then amplitude death is never induced for any connection parameter and network topology. In such a case, we must change $\boldsymbol{b}, \boldsymbol{c}$ or give up on inducing death.

3.2. Stable conditions

Here, we show some necessary conditions to ensure that equilibrium state (3) is stable. First, we introduce segment polynomial $L(z)$ as follows:

$$L(z) := \{g(z,\rho) : \rho \in [0,\bar{\rho}]\}, \tag{15}$$

where $\bar{\rho} \leq 2$ is the upper limit of the maximum eigenvalue ρ_N in inequality (9). Note that ρ in polynomial (14) depends on $\boldsymbol{E}$ and N. In addition, the segment polynomial (15) can be rewritten by a function of a parameter μ as follows:

$$L(z) = \{g(z,0) + \mu\hat{g}(z) : \mu \in [0,1]\}, \tag{16}$$

where

$$\hat{g}(z) := g(z,\bar{\rho}) - g(z,0) \tag{17}$$

denotes the direction of the segment.

This segment polynomial can be used for analysis of the local stability of equilibrium state (3).

Corollary 3. *If $L(z)$ is stable[3], then equilibrium state (3) is locally stable for any network whose ρ_N is less than or equal to $\bar{\rho}$.*

Proof. The polynomials $g(z,\rho_q)$ $(q = 1,\ldots,N)$ for coupled map networks whose ρ_N is less than or equal to $\bar{\rho}$ are a subset of $L(z)$. This suggests that if $L(z)$ is stable, then equilibrium state (3) in the coupled map networks is stable locally. □

[3] A segment is stable if and only if every polynomial on the segment is stable [47].

The following lemma gives the necessary condition for $L(z)$ to be stable.

Lemma 4. *The fact that two polynomials, i.e.,*

$$d(z) + kn(z), \tag{18}$$

$$z^{\tau} d(z) + kn(z)(z^{\tau} - 1), \tag{19}$$

are stable is a necessary condition for $L(z)$ to be stable.

Proof. It has been reported [30] that the maximum eigenvalue ρ_N satisfies the following:

$$1 < \frac{N}{N-1} \leq \rho_N \leq 2. \tag{20}$$

Thus, $1 < \rho_N$ always holds. Then $L(z)$ must include $g(z, 1) = z^{\tau} \{d(z) + kn(z)\}$. Furthermore, we have $\rho_1 = 0$; thus, $g(z, 0)$ must also be an element of $L(z)$. Consequently, each stability is a necessary condition for $L(z)$ to be stable. As can be seen, the stability of $g(z, 1)$ and $g(z, 0)$ is equal to that of polynomials (18) and (19), respectively. □

We see that polynomial (18) is the same as the characteristic polynomial of a control system with a forward plant $n(z)/d(z)$ and negative feedback part k. Note that polynomial (19) depends on τ, but polynomial (18) does not. This fact suggests an order for designing k and τ. First, a range of k is derived from polynomial (18). Second, τ is chosen such that polynomial (19) is stable within the range of k.

The robust control theory provides a sufficient condition under which $L(z)$ is stable.

Lemma 5 (Ref. [37])**.** *Segment polynomial $L(z)$ in Eq. (16) is stable if all of the following are satisfied.*

(c-1) *$g(z, 0)$ is a stable polynomial,*

(c-2) *$g(z, \bar{\rho})$ is a stable polynomial,*

(c-3) *$\hat{g}(z)$ is a convex direction (see Appendix A).*

Conditions (c-1) and (c-2) can be checked by a popular stability analysis method [48]. The direction in condition (c-3) can be simplified as follows:

$$\hat{g}(z) = g(z, \bar{\rho}) - g(z, 0) = \bar{\rho} kn(z). \tag{21}$$

Note that the direction depends on only $n(z)$. From Theorem 3 in Appendix A, we have a simple condition for the direction.

Lemma 6. *A real polynomial $\hat{g}(z)$ is a convex direction if the following inequality holds:*

$$\frac{1}{n_r(\theta)^2 + n_i(\theta)^2} \left(n_r(\theta) \frac{\mathrm{d}n_i(\theta)}{\mathrm{d}\theta} - n_i(\theta) \frac{\mathrm{d}n_r(\theta)}{\mathrm{d}\theta} \right) \leq \frac{m}{2}, \ \theta \in (0, \pi), \tag{22}$$

where $n\left(e^{j\theta}\right) := n_r(\theta) + jn_i(\theta)$.

Proof. From Theorem 3 in Appendix A, we note that a sufficient condition for $\hat{g}(z)$ to be a convex direction is that the following inequality holds.

$$\frac{\partial \arg\left\{\hat{g}\left(e^{j\theta}\right)\right\}}{\partial \theta} \leq \frac{m}{2}, \ \theta \in (0, \pi) \tag{23}$$

Substituting $n\left(e^{j\theta}\right) := n_r(\theta) + jn_i(\theta)$ and Eq. (21) into inequality (23) yields inequality (22). □

These sufficient and necessary conditions and the stability analysis on the convex direction will be used in the design of the connection parameters and the input-output matrices of maps in the next section.

4. Design for inducing amplitude death

Here, we show a procedure to design the connection parameters (i.e., k and τ) and input-output matrices (i.e., $\boldsymbol{b}$ and $\boldsymbol{c}$) to induce stabilization on the basis of our analytical results discussed in the preceding section (Fig. 2).

(Step 0) Compute $\boldsymbol{A}$. Assume that matrix $\boldsymbol{A}$ is unstable (Assumption 1).

(Step 1) If an odd number of eigenvalues of matrix $\boldsymbol{A}$ are on the real axis and greater than one, quit the design; otherwise, proceed to the next step (Theorem 1).

(Step 2) $\boldsymbol{b}$ and $\boldsymbol{c}$ are set to new matrices such that $(\boldsymbol{A}, \boldsymbol{b}, \boldsymbol{c})$ is minimal.

(Step 3) If $n(z) = \boldsymbol{c}\mathrm{adj}(z\boldsymbol{I}_m - \boldsymbol{A})\boldsymbol{b}$ satisfies inequality (22), then proceed to the next step; otherwise, return to (Step 2) or quit the design ((c-3) in Lemma 5 and Lemma 6).

(Step 4) Calculate the zeros $\hat{z}$ of $n(\hat{z}) = 0$. If we find at least one $\hat{z} > 1$ such that an odd number of eigenvalues of the matrix $\boldsymbol{A}$ are on the real axis and are greater than the zero $\hat{z} > 1$, then return to (Step 2) or quit the design; otherwise, proceed to the next step (Corollary 1).

(Step 5) For an even (odd) m, if we find at least one $\hat{z} < -1$ such that an odd (even) number of eigenvalues of the matrix $\boldsymbol{A}$ are on the real axis and are greater than the zero $\hat{z} < -1$, then return to (Step 2) or quit the design; otherwise, proceed to the next step (Corollary 2).

(Step 6) Derive the range of gain k such that polynomial (18) is stable ((c-1) in Lemma 5). If the range exists, then proceed to the next step; otherwise, return to (Step 2) or quit the design (Lemma 4).

(Step 7) If an odd (even) number of eigenvalues of the matrix $\boldsymbol{A}$ are on the real axis and are greater than -1 for an even (odd) m, then $\tau > 0$ is set to a new odd number; otherwise, it is set to a new number (Theorem 2). Proceed to the next step.

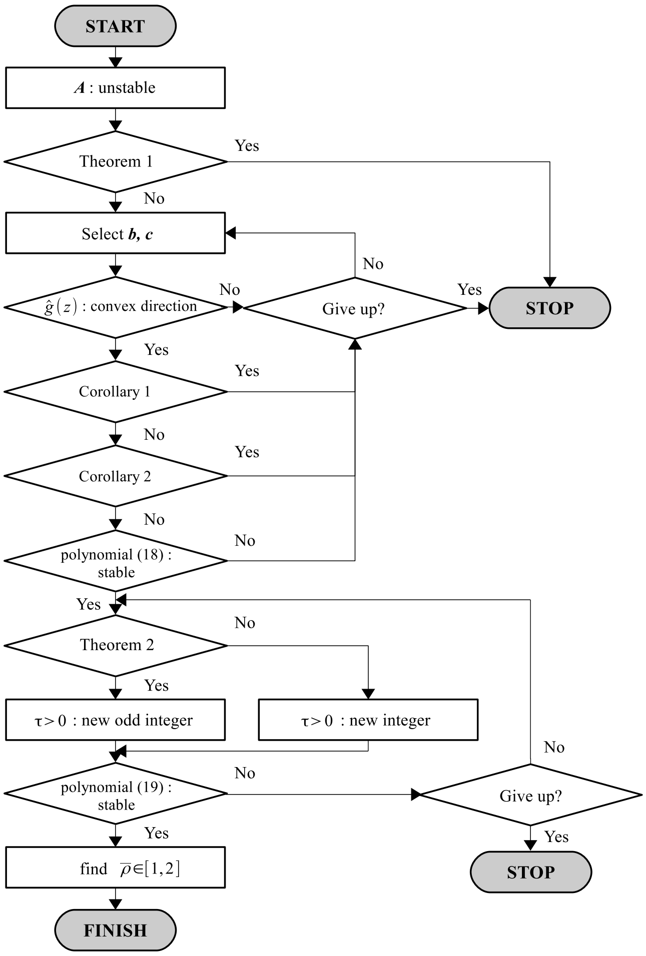

Figure 2: Design procedure of k, τ, $\boldsymbol{b}$, and $\boldsymbol{c}$ for inducing amplitude death

(Step 8) Derive the range of k where polynomial (19) is stable. If there exists a partial overlap between the ranges in (Step 6) and (Step 8), then proceed to the next step; otherwise, return to (Step 7) or quit the design (Lemma 4).

(Step 9) For k within the overlap range, find $\bar{\rho} \in [1, 2]$ such that $g(z, \bar{\rho})$ is a stable polynomial ((c-2) in Lemma 5).

This procedure appears difficult because it has 10 steps. However, most steps can be checked easily. These steps reduce the burden of design.

5. Numerical examples

Here, we confirm our analytical results using three types of maps in numerical simulations.

5.1. Delayed logistic map networks

The following delayed logistic map [38, 39] is used as nonlinear map $\boldsymbol{F}$ with $m = 2$ in Eq. (1).

$$\boldsymbol{F}(\boldsymbol{x}) := \begin{bmatrix} x_{(2)} \\ 2.1x_{(2)}\{1 - x_{(1)}\} \end{bmatrix} \tag{24}$$

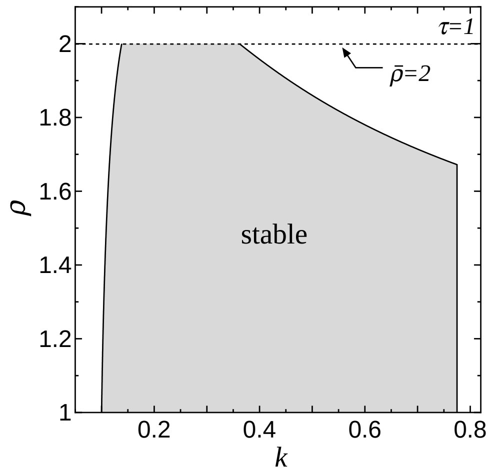

Figure 3: Stable region of $g(z, \rho)$ for delayed logistic map (24) networks

The fixed points of this map are described by $\boldsymbol{x}_a^* = [0\ 0]^T$ and $\boldsymbol{x}_b^* = [0.5238\ 0.5238]^T$. In accordance with the proposed procedure, we design parameters k, τ, $\boldsymbol{b}$, and $\boldsymbol{c}$ as follows.

For (Step 0), we see that $\boldsymbol{x}_{a,b}^*$ are unstable because the eigenvalues of $\{\boldsymbol{A}\}_{\boldsymbol{x}=\boldsymbol{x}_{a,b}^*}$ are $\lambda = 0, 2.1$ and $\lambda = 1/2 \pm j\sqrt{3.4}/2$, respectively. For (Step 1), the eigenvalues of $\{\boldsymbol{A}\}_{\boldsymbol{x}=\boldsymbol{x}_a^*}$ satisfy the odd number property; thus, amplitude death does not occur at $\boldsymbol{x}_a^*$. In contrast, for another fixed point $\boldsymbol{x}_b^*$, the eigenvalues of $\{\boldsymbol{A}\}_{\boldsymbol{x}=\boldsymbol{x}_b^*}$ do not satisfy the property. Therefore, we focus on $\boldsymbol{x}_b^*$. For (Step 2), $\boldsymbol{b} = [1\ 0]^T$ and $\boldsymbol{c} = [1\ 0]$ are fixed. It is easy to check numerically that $(\boldsymbol{A}, \boldsymbol{b}, \boldsymbol{c})$ is minimal. For (Step 3), we have $n(z) = z - 1$, which satisfies inequality (22). For (Step 4), we see that there does not exist the zero $\hat{z} > 1$ of $n(\hat{z}) = 0$. For (Step 5), we also see that there does not exist the zero $\hat{z} < -1$ of $n(\hat{z}) = 0$. For (Step 6), we analytically find that polynomial (18) is stable for $k \in (0.1000, 1.5500)$. For (Step 7), as in (Step 0), the matrix $\{\boldsymbol{A}\}_{\boldsymbol{x}=\boldsymbol{x}_b^*}$ does not have real eigenvalues greater than -1. Thus, delay time τ can be set to an arbitrary number; we select $\tau = 4$. For (Step 8), we cannot numerically determine k for polynomial (19) to be stable. Therefore, we return to (Step 7) and reset it to $\tau = 1$. We analytically obtain the stable range $k \in (0.1000, 0.7750)$. The overlap range in (Step 6) and (Step 8) is $k \in (0.1000, 0.7750)$. For (Step 9), we find the largest possible $\rho \in [1, 2]$, i.e., $\bar{\rho}$, such that $g(z, \bar{\rho})$ is stable. The gain range within the overlap range for $g(z, \rho)$ to be stable is estimated numerically as ρ varies from 1 to 2 (Fig. 3). We find $\bar{\rho} = 2$, and this fact indicates that the stabilization of equilibrium state (3) occurs for any network $\boldsymbol{E}$.

Using numerical simulations, we confirm that the designed parameters induce the stabilization of state (3) in two types of networks with eight maps ($N = 8$), i.e., an all-to-all network and a ring network on two nearest neighbors (Fig. 4). From Fig. 3, we choose $k = 0.3$. Figures 4 (a) and (b) show time-series data of the first variables in system states $\boldsymbol{x}_i := [x_{(1)i}\ x_{(2)i}]^T$ $(i = 1, \ldots, 8)$ for the all-to-all network and the ring network, respectively. For $n < 100$, each map without connection $(k \equiv 0)$ behaves independently. These maps are connected at $n = 100$.

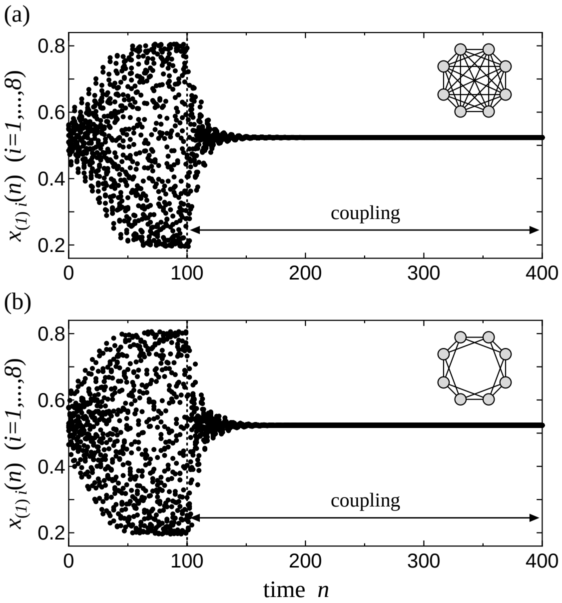

Figure 4: Time-series data of the first variables in system states $\boldsymbol{x}_i := [x_{(1)i}\ \ x_{(2)i}]^T$ ($i = 1, \ldots, 8$) with the designed parameters ($k = 0.3$, $\tau = 1$, $\boldsymbol{b} = [1\ 0]^T$, $\boldsymbol{c} = [1\ 0]$) for delayed logistic map (24) networks: (a) all-to-all network and (b) ring network with two nearest neighbors

As can be seen, all maps converge on the fixed point $\boldsymbol{x}_b^*$. These results indicate that the stabilization of state (3) is induced successfully by the designed parameters.

5.2. Generalized Henon map networks

Consider a generalized Henon map with $m = 3$ [40] with two fixed points, i.e., $\boldsymbol{x}_a^* = [0.5235\ 0.5235\ 0.5235]^T$ and $\boldsymbol{x}_b^* = [-1.6235\ -1.6235\ -1.6235]^T$.

$$\boldsymbol{F}(\boldsymbol{x}) := \begin{bmatrix} 0.85 - x_{(2)}^2 - 0.1x_{(3)} \\ x_{(1)} \\ x_{(2)} \end{bmatrix} \tag{25}$$

For (Step 0), $\boldsymbol{x}_{a,b}^*$ are unstable because their eigenvalues are $\lambda = -0.0947, 0.0473 \pm j1.0266$ and $\lambda = -1.8172, 0.0308, 1.7864$. The odd number property holds at $\boldsymbol{x}_b^*$; however, this property does not hold at $\boldsymbol{x}_a^*$. For (Step 2), $\boldsymbol{b} = [1\ 0\ 0]^T$ and $\boldsymbol{c} = [1\ 0\ 0]$ are set, and then $(\boldsymbol{A}, \boldsymbol{b}, \boldsymbol{c})$ is minimal. For (Step 3), $n(z) = z^2$ does not satisfy inequality (22). Return to (Step 2). For (Step 2), $\boldsymbol{b} = [0\ 1\ 0]^T$ and $\boldsymbol{c} = [1\ 0\ 0]$ are set, and then $(\boldsymbol{A}, \boldsymbol{b}, \boldsymbol{c})$ is minimal. For (Step 3), $n(z) = \left(1.1 - \sqrt{461}/10\right) z - 0.1$ satisfies inequality (22). For (Step 4), $n(\hat{z}) = 0$ does not have the zero $\hat{z} > 1$. For (Step 5), $n(\hat{z}) = 0$ does not have the zero $\hat{z} < -1$. For (Step 6), polynomial (18) is stable for $k \in [0.0536, 1.8717]$. For (Step 7), we see that $\boldsymbol{A}$ has one real eigenvalue $\lambda = -0.0947$ greater than -1 for odd $m = 3$. Thus, $\tau = 4$ is set. For (Step 8), we find no stable range of k and return to (Step 7), where $\tau = 2$ is set. Consequently, we have the stable range $k \in [0.0269, 0.8900]$. The overlap range is $k \in [0.0536, 0.8900]$. For (Step 9), we numerically find $\bar{\rho} = 1.944$, as shown in Fig. 5. These steps suggest that the stabilization of equilibrium state (3) can occur for any $\boldsymbol{E}$ under the restriction of $\rho_N \le \bar{\rho} = 1.944$.

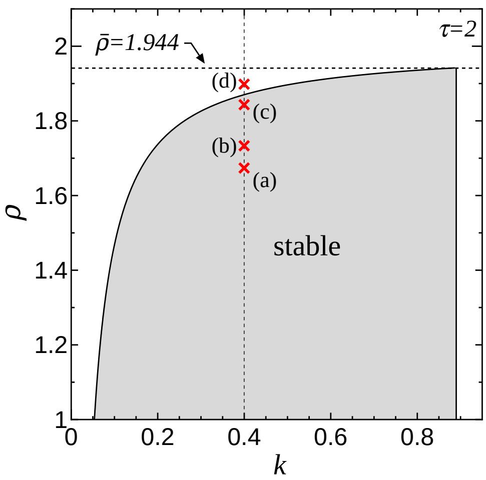

Figure 5: Stable region of $g(z, \rho)$ for generalized Henon map (25) networks

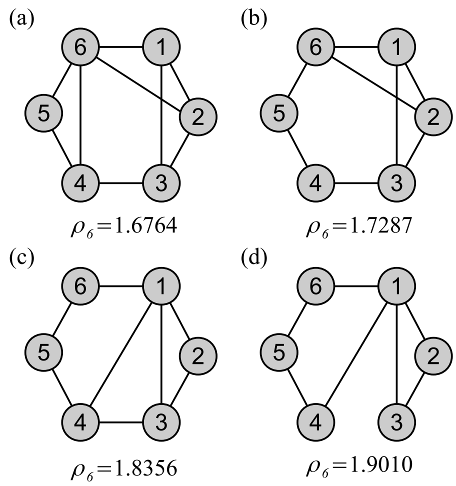

Figure 6: Four types of network topology and their ρ_6: networks (a), (b), (c), and (d) correspond to the same label in Fig. 5

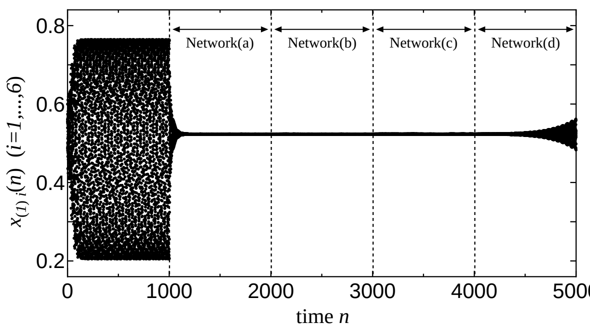

Figure 7: Time-series data of the first variables in system states $\boldsymbol{x}_i := [x_{(1)i}\ \ x_{(2)i}]^T$ ($i = 1, \ldots, 6$) with the designed parameters ($k = 0.4$, $\tau = 2$, $\boldsymbol{b} = [0\ 1\ 0]^T$, and $\boldsymbol{c} = [1\ 0\ 0]$) for the four types of Henon map (25) network consisting of six maps ($N = 6$) shown in Fig. 6

To confirm the designed parameters numerically, we employ four types of networks consisting of the six maps ($N = 6$) shown in Fig. 6. According to the above steps, parameters $k = 0.4$, $\tau = 2$, $\boldsymbol{b} = [0\ 1\ 0]^T$, and $\boldsymbol{c} = [1\ 0\ 0]$ are fixed. As can be seen from Fig. 5, the designed parameters can induce the stabilization for networks (a), (b), and (c). This fact suggests that the stabilization can be maintained even when the connections in the network are rewired at long intervals. In other words, the stabilization is robust against such network rewiring, and our analysis is useful to know the permitted types of rewiring. Figure 7 shows the time series data[4] of all the maps when the network topology is switched as follows: no connection for $n \in [0, 1000)$, the network in Fig.6 (a) for $n \in [1000, 2000)$, the network in Fig.6 (b) for $n \in [2000, 3000)$, the network in Fig.6 (c) for $n \in [3000, 4000)$, and the network in Fig.6 (d) for $n \in [4000, 5000)$. As can be seen, all maps that behave oscillatory without connection converge on equilibrium state (3) for networks (a), (b), and (c) but behave oscillatory again for network (d). These numerical results agree well with our analysis.

5.3. Piecewise linear map networks

is used: Here, the following piecewise linear map with $m = 3$ [41, 42]

$$\boldsymbol{F}(\boldsymbol{x}) := \begin{bmatrix} f(x_{(1)}, 1.9) + 0.4x_{(2)} - 0.5x_{(3)} \\ 0.1x_{(1)} + f(x_{(2)}, 1.8) \\ 0.1x_{(1)} - 0.2x_{(3)} \end{bmatrix}, \tag{26}$$

where

$$f(x, p) = \begin{cases} p(x+1) & (x < -0.5) \\ px & (-0.5 \le x \le 0.5) \\ p(x-1) & (0.5 < x) \end{cases}.$$

This map has seven fixed points. Note that all the points have the same Jacobi matrix $\boldsymbol{A}$.

For (Step 0), the matrix $\boldsymbol{A}$, which has the eigenvalues $\lambda = -0.1757$, 1.6331, and 2.0426, is unstable. For (Step 1), $\boldsymbol{A}$ has two real eigenvalues greater than 1; thus, the odd number property is not satisfied. For (Step 2), $\boldsymbol{b} = [1\ 0\ 0]^T$ and $\boldsymbol{c} = [0\ 0\ 1]$ are set. $(\boldsymbol{A}, \boldsymbol{b}, \boldsymbol{c})$ is minimal. For (Step 3), $n(z) = 0.1(z - 1.8)$ satisfies inequality (22). For (Step 4), as can be seen, there exists one real eigenvalue $\lambda = 2.0426$ greater than the zero $\hat{z} = 1.8$ of $n(\hat{z}) = 0$. Thus, return to (Step 2). For (Step 2), $\boldsymbol{b} = [1\ 0\ 0]^T$ and $\boldsymbol{c} = [0\ 1\ 0]$ are set, and we confirm that $(\boldsymbol{A}, \boldsymbol{b}, \boldsymbol{c})$ is minimal. Proceed to (Step 3). For (Step 3), $n(z) = 0.1(z + 0.2)$ satisfies inequality (22). For (Step 4), $n(\hat{z}) = 0$ does not have the zero $\hat{z} > 1$. For (Step 5), $n(\hat{z}) = 0$ does not have the zero $\hat{z} < -1$. For (Step 6), we cannot find the stable range of k for polynomial (18), and give up the design of $(k, \tau, \boldsymbol{b}, \boldsymbol{c})$.

[4]The small uniformly distributed random noises within $\left[-1.0 \times 10^{-4}, 1.0 \times 10^{-4}\right]$ are added to all maps to confirm the local stability of the equilibrium state (3).

6. Discussion

This section accurately surveys the relationship between the present study and previous studies on amplitude death in discrete-time map networks. In addition, we briefly discuss bifurcation analysis.

Masoller and Martí observed that amplitude death can occur in one-dimensional map networks with random delay connections [31]. Their results have been investigated analytically in view of multiple delayed feedback control [32] and examined numerically for regular and random topologies [33, 35]. Gong *et al.* investigated amplitude death in one-dimensional map networks with distributed delay connections analytically and numerically [34]. Han reported oscillation death in coupled one-dimensional maps with local and global no-delay connections [49]. Masoller and Atay investigated transitions between an oscillatory synchronization state and an amplitude death state in one-dimensional map networks with delay connections [50]. Shekatkar and Ambika proposed a dynamic lattice for stabilizing coupled high-dimensional map lattices [51]. Based on the characteristic polynomial (10) with $m = 1$, Atay and Karabacak [30] provided the necessary and sufficient condition under which amplitude death occurs in one-dimensional map networks with uniform delay connections. This condition revealed the following: (i) amplitude death never occurs for $\rho_N = 2$ and (ii) odd time delays can induce amplitude death but not for even time delays. Fact (i) agrees with our previous study [28]. Note that fact (ii), which was also mentioned in a previous study [32], is invalid for high-dimensional map networks, as discussed in Subsection 5.2. Moreover, study [30] mentioned stability analysis for high-dimensional map networks. Our conference paper [36] dealt with high-dimensional map networks with uniform delay time and provided a primitive procedure for designing only the connection parameters. This primitive procedure required heavy trial-and-error tasks when designing connections. On the other hand, the present paper provides an advanced procedure for designing connection parameters and the input-output matrices. This procedure does not require such heavy trial-and-error tasks because we find several sufficient conditions for instability and necessary conditions for stability.

This paper has dealt with only the stability analysis of equilibrium state (3) and the design procedure for stabilization; however, we did not examine them from the viewpoints of bifurcation theory. Our concern is to reveal the stabilization mechanism of equilibrium state (3). Our conference paper numerically observed the stabilization induced via the Neimark-Sacker bifurcation and the period-doubling bifurcation [52], while bifurcation analysis of the stabilization is still lacking.

7. Conclusion

We have analytically investigated amplitude death in networks consisting of one or more dimensional nonlinear maps with time delay connections. We have demonstrated that the well-known odd number property remains in map networks. We have obtained several sufficient conditions for death state to be unstable. Some necessary conditions for stability and the concept of the convex direction have been also derived. Based on our analytical results, a design procedure for system parameters, which consists of 10 steps, has been provided. This procedure has been confirmed by three numerical examples, i.e., networks with delayed logistic maps, three-dimensional generalized Henon maps, and three-dimensional piecewise linear maps.

Acknowledgments

This research was partially supported by The Telecommunications Advancement Foundation and JSPS KAKENHI (26289131).

Appendix A. Convex direction

Consider the following family of m-order polynomials:

$$\begin{aligned} \delta(z) &= \{\mu\delta_1(z) + (1-\mu)\delta_2(z) : \mu \in [0,1]\}, \\ &= \left\{\delta_2(z) + \mu\hat{\delta}(z) : \mu \in [0,1]\right\}, \end{aligned} \tag{A.1}$$

where $\hat{\delta}(z) := \delta_1(z) - \delta_2(z)$ is a polynomial whose degree is less than m. For family (A.1), the convex direction is defined as follows:

Definition 1 ([37, 53]). *A polynomial $\hat{\delta}(z)$ is called a convex direction for stable polynomials of degree m if, for every polynomial $\delta_2(z)$, the stability of $\delta_2(z)$ and $\delta_2(z) + \hat{\delta}(z)$ implies the stability of the family $\delta(z)$.*

From this definition, we note that if the edges of the family $\delta_{1,2}(z)$ are stable and $\hat{\delta}(z)$ is a convex direction, then the family $\delta(z)$ is stable. Although the stability of $\delta_{1,2}(z)$ can be checked easily by some popular analytical tools, it is difficult to check the convex direction of $\hat{\delta}(z)$. A simple checking procedure is given below.

Theorem 3 ([37, 53]). *If the inequality*

$$\frac{\partial \arg\left\{\hat{\delta}\left(e^{j\theta}\right)\right\}}{\partial\theta} \leq \frac{m}{2} + \left|\frac{\sin\left(2\arg\left\{\hat{\delta}\left(e^{j\theta}\right)\right\} - m\theta\right)}{2\sin\theta}\right|, \tag{A.2}$$

$$\theta \in \left\{\phi \in (0,\pi); \hat{\delta}\left(e^{j\phi}\right) \neq 0\right\}, \tag{A.3}$$

holds, then $\hat{\delta}(z)$ is a convex direction.

References

[1] S.H. Strogatz, Sync: The emerging science of spontaneous order, 1st Edition, Hyperion Books, New York, 2003.
[2] A. Pikovsky, M. Rosenblum, and J. Kurths, Synchronization, Cambridge University Press, 2001.
[3] S. Boccaletti, V. Latora, Y. Moreno, M. Chavez, and D.U. Hwang, Complex networks: Structure and dynamics, Phys. Rep. 424 (2006) 175 – 308.
[4] G. Osipov, J. Kurths, and C. Zhou, Synchronization in oscillatory networks, Springer, 2007.
[5] K. Kaneko, Overview of coupled map lattices, Chaos 2 (1992) 279–282.
[6] K. Kaneko, Theory and applications of coupled map lattices, Wiley, Chichester, England, 1993.
[7] A. Arenas, A. Diaz-Guilera, J. Kurths, Y. Moreno, and C. Zhou, Synchronization in complex networks, Phys. Rep. 469 (2008) 93 – 153.
[8] F. Dorfler and F. Bullo, Synchronization in complex networks of phase oscillators: A survey, Automatica 50 (2014) 1539 – 1564.
[9] G. Saxena, A. Prasad, and R. Ramaswamy, Amplitude death: The emergence of stationarity in coupled nonlinear systems, Phys. Rep. 521 (2012) 205 – 228.
[10] A. Koseska, E. Volkov, and J. Kurths, Oscillation quenching mechanisms: Amplitude vs. oscillation death, Phys. Rep. 531 (2013) 173 – 199.
[11] D.Q. Wei, B. Zhang, X.S. Luo, S.Y. Zeng, and D.Y. Qiu, Effects of couplings on the collective dynamics of permanent-magnet synchronous motors, IEEE Trans. Circuits and Sys. II 60 (2013) 692–696.
[12] S. Huddy and J. Skufca, Amplitude death solutions for stabilization of DC microgrids with instantaneous constant-power loads, IEEE Trans. Power Electronics 28 (2013) 247 –253.
[13] T. Biwa, S. Tozuka, and T. Yazaki, Amplitude death in coupled thermoacoustic oscillators, Phys. Rev. Applied 3 (2015) 034006.
[14] D. Aronson, G. Ermentrout, and N. Kopell, Amplitude response of coupled oscillators, Physica D 41 (1990) 403–449.
[15] K. Konishi, Limitation of time-delay induced amplitude death, Phys. Lett. A 341 (2005) 401–409.
[16] D. Reddy, A. Sen, and G. Johnston, Time delay induced death in coupled limit cycle oscillators, Phys. Rev. Lett. 80 (1998) 5109–5112.
[17] S. Strogatz, Death by delay, Nature 394 (1998) 316–317.
[18] K. Konishi, Amplitude death induced by dynamic coupling, Phys. Rev. E 68 (2003) 067202.
[19] K. Konishi, Amplitude death induced by a global dynamic coupling, Int. J. Bifurcation and Chaos 17 (2007) 2781–2789.
[20] K. Konishi and N. Hara, Topology-free stability of a steady state in network systems with dynamic connections, Phys. Rev. E 83 (2011) 036204.
[21] R. Karnatak, R. Ramaswamy, and A. Prasad, Amplitude death in the absence of time delays in identical coupled oscillators, Phys. Rev. E 76 (2007) 035201.
[22] W. Zou, D. Senthilkumar, M. Zhan, and J. Kurths, Reviving oscillations in coupled nonlinear oscillators, Phys. Rev. Lett. 111 (2013) 014101.
[23] J. Hofener, G. Sethia, and T. Gross, Amplitude death in networks of delay-coupled delay oscillators, Phil. Trans. Roy. Soc. A 371 (2013) 20120462.
[24] W. Zou, D. Senthilkumar, Y. Tang, Y. Wu, J. Lu, and J. Kurths, Amplitude death in nonlinear oscillators with mixed time-delayed coupling, Phys. Rev. E 88 (2013) 032916.
[25] Y. Kyrychko, K. Blyuss, and E. Schöll, Amplitude and phase dynamics in oscillators with distributed-delay coupling, Phil. Trans. Roy. Soc. A 371 (2013) 20120466.
[26] W. Just, A. Pelster, M. Schanz, and E. Schöll, Delayed complex systems: An overview, Phil. Trans. R. Soc. A 368 (2010) 303 – 304.
[27] V. Flunkert, I. Fischer, and E. Schöll, Dynamics, control and information in delay-coupled systems: An overview, Phil. Trans. R. Soc. A 371 (2013) 20120465.
[28] K. Konishi, Time-delay-induced stabilization of coupled discrete-time systems, Phys. Rev. E 67 (2003) 017201.
[29] K. Konishi and H. Kokame, Time-delay-induced amplitude death in chaotic map lattices and its avoiding control, Phys. Lett. A 366 (2007) 585–590.
[30] F.M. Atay and O. Karabacak, Stability of coupled map networks with delays, SIAM J. Appl. Dyn. Syst. 5 (2006) 508–527.
[31] C. Masoller and A.C. Marti, Random delays and the synchronization of chaotic maps, Phys. Rev. Lett. 94 (2005) 134102.
[32] A.C. Marti, M. Ponce, and C. Masoller, Steady-state stabilization due to random delays in maps with self-feedback loops and in globally delayed-coupled maps, Phys. Rev. E 72 (2005) 066217.
[33] A.C. Marti, M. Ponce, and C. Masoller, Chaotic maps coupled with random delays: Connectivity, topology, and network propensity for synchronization, Physica A 371 (2006) 104 – 107.
[34] X. Gong, S. Guan, X. Wang, and C.H. Lai, Stability of the steady state of delay-coupled chaotic maps on complex networks, Phys. Rev. E 77 (2008) 056212.
[35] M. Ponce, C. Masoller, and A.C. Marti, Synchronizability of chaotic logistic maps in delayed complex networks, Eur. Phys. J. B 67 (2009) 83–93.
[36] T. Watanabe, Y. Sugitani, K. Konishi, and N. Hara, Amplitude death in high-dimensional map networks with connection delays, Proc. of International Symposium on Nonlinear Theory and its Applications (2014) 719–722.

[37] L. Atanassova, D. Hinrichsen, and V. Kharitonov, Convex directions for stable polynomials and quasipolynomials: A survey of recent results, in: L. Dugard, E. Verriest (Eds.), Stability and Control of Time-delay Systems, Vol. 228 of Lecture Notes in Control and Information Sciences, Springer, 1998, pp. 72–91.

[38] J. Guckenheimer and P. Holmes, Nonlinear oscillations, dynamical systems, and bifurcations of vector fields, Springer-Verlag, New Yorke, USA, 1983.

[39] J. Thompson and H. Stewart, Nonlinear dynamics and chaos, Wiley, New York, 2001.

[40] H. Richter, The generalized Henon maps: Examples for higher-dimensional chaos, Int. J. Bifurcation and Chaos 12 (2002) 1371–1384.

[41] K. Konishi and H. Kokame, Observer-based delayed-feedback control for time-discrete chaotic systems, Phys. Lett. A 248 (1998) 359 – 368.

[42] S. Yamamoto, T. Hino, and T. Ushio, Delayed feedback control with a minimal-order observer for stabilization of chaotic discrete-time systems, Int. J. Bifurcation and Chaos 12 (2002) 1047–1055.

[43] C. Chui, C. K, and G. Chen, Discrete H^∞ optimization, Springer-Verlage, 1997.

[44] L. B. Le, K. Konishi, and N. Hara, Topology-free design for amplitude death in time-delayed oscillators coupled by a delayed connection, Phys. Rev. E 87 (2013) 042908.

[45] T. Ushio, Limitation of delayed feedback control in nonlinear discrete-time systems, IEEE Trans. Circuits and Sys. I 43 (1996) 815–816.

[46] K. Konishi, M. Ishii, and H. Kokame, Stability of extended delayed-feedback control for discrete time chaotic systems, IEEE Trans. Circuits and Sys. I 46 (1999) 1285–1288.

[47] S. Bhattacharyya, H. Chapellat, and L. Keel, Robust control: The parametric approach, Prentice Hall PTR, NJ, 1995.

[48] K. Ogata, Discrete-time control systems, Pearson Education, 1994.

[49] Y.J. Han, Steady states of globally and locally coupled maps, J. Korean Phys. Soc. 56 (2010) 697–703.

[50] C. Masoller and F. Atay, Complex transitions to synchronization in delay-coupled networks of logistic maps, Eur. Phys. J. D 62 (2011) 119–126.

[51] S.M. Shekatkar and G. Ambika, Novel coupling scheme to control dynamics of coupled discrete systems, Commun. Nonlinear Sci. Numer. Simul. 25 (2015) 50 – 65.

[52] T. Watanabe, Y. Sugitani, K. Konishi, and N. Hara, Stabilization mechanism of amplitude death in a high-dimensional map network with a connection delay, Proc. of IFAC Conference on Analysis and Control of Chaotic Systems 48 (2015) 163–168.

[53] D. Hinrichsen and V. Kharitonov, On convex directions for stable polynomials, Autom. Rem. Contr. 58 (1997) 394–402.